Response to Reviewer#2 TC-2022-123

Review of "Simulation of the current and future dynamics of permafrost near the northern limit of permafrost on the Qinghai–Tibet Plateau" By Zhao et al.

Climate warming has undoubtedly impacted the Cryospheric over the Tibetan Plateau. As the most

widely distributed cryosphere element, thawed permafrost has caused damage to the natural and social economy; therefore, projections of the permafrost dynamics are the primary step to mitigating and adapting to climate change. Aiming to understand the permafrost dynamics on the regional scale, a model is a more powerful tool than fieldwork. Here, Zhao et al. apply a one-dimension heat conduction model to detect the permafrost change located on the permafrost's northern edge over the Tibetan Plateau. After evaluating the model's performance based on borehole records, the authors investigated the permafrost dynamics under historical and future climate conditions and claimed the terrain strongly affected the thermal regime of permafrost in the Xidatan area.

In general, this work should deserve attention or consideration by The Cryosphere if the authors

could address review comments and add additional information.

Response:

Thanks a lot for the comments on our paper, which helped us to improve the quality of the manuscript. Following is our detail response to those comments and describe how we addressed these our revised manuscript according to the CCs request data. The original reviewer comments are in normal black font while our answers appear in bule font. The corresponding edit in the manuscript are included in red font.

General comments:

1. It is hard for me to understand the approach that the authors applied to generate the forcing data for the future period (last paragraph of section 2.3.3). Firstly, why do authors regard the warming climate rate in the Xidatan Area as equal to the warming rate over the Tibetan Plateau in the future? In other words, why the mean warming rate of the larger area (e.g., Tibetan Plateau) can represent that of the smaller area (e.g., Xidatan area)? Secondly, if I understand the function (Eq 8 in Sun et al., 2019) which calculates the daily land surface temperature correctly, why do the authors consider the forcing data (land surface temperature) is linearly increasing in the future? Perhaps, the results of future projections in this manuscript may overestimate the permafrost degradation conditions in the future.

Response:

We share the reviewer's concern as well which was discussed at length by the authors during the study's design.

Firstly, considerable studies have evaluated the performance of the CMIP5/CMIP6 model in simulating temperature over the QTP during the 21st century (You et al., 2021; Lun et al., 2021;

Gui et al., 2021; Zhu et al., 2020; Jia et al., 2019; Hu et al., 2014). Their results suggest that much large discrepancies and uncertainties appeared between GCM/regional climate model (RCM) historical period simulations and observed climate on the QTP due to the high and complex topography, the vagaries of the local climate environment, the sparseness of meteorological stations on the plateau (You et al., 2021; Su et al., 2013; Chen et al., 2017). Historical climate simulations are not reliable how for accurately estimating future projections. Moreover, overly coarse model resolution (typically on the order of several degrees of latitude/ longitude or coarser spatial resolution) to capture the more detailed regional information which has been identified as important in determining the QTP climatology (Zhu et al.,2013; Gao et al., 2008). Furthermore, these coarse resolutions are difficult to match well, and are not suitable for regional or smaller scales permafrost and climate change assessment. Therefore, an adaptation of results from GCM/RCM runs to the small-area and marginal permafrost, like Xidatan, is highly problematic, which leads to an inaccurate projection of permafrost. The primary objective of this study was realistically simulation the distribution of marginal permafrost on the QTP, thereby quantitatively assess historical (1970-2019) evolution process of mountain permafrost in the northern lower limit of the permafrost zone (Xidatan) on the QTP. Our model is validated at several sites throughout Xidatan against observations, we consistently reproduced the vertical ground temperature profile and active layer thickness for the last 10 years, and are superior in recognizing permafrost boundaries, and the present permafrost distribution is reproduced when simulating the evolution since 1970. This gives us confidence that our simulation results can capture the dominating process of heat transfer in permafrost and accurately reflect the lagging response of permafrost to climate change. We anticipated the possible fate of permafrost over our study area by 2100 under RCP and SSP scenarios. These scenarios are an area-mean warming rate of QTP and are derived from the latest IPCC AR6 evaluations (IPCC, 2021; Iturbide ET AL., 2020). We believe our simulation results can provide a relatively reasonable projection indication of the permafrost degradation levels over whole permafrost on the QTP under the different climate change scenarios in the foreseeable future. Unquestionable, reasonable, and high-quality air temperature projection is a need for a more credible projection of permafrost degradation. In future modeling efforts, high-resolution climate models and improved numerical representations of atmospheric circulation systems and land-atmosphere interactions over the heterogeneous QTP region could be one of the crucial steps toward improving the accuracy of permafrost degradation projections.

Secondly, the near-surface ground temperature is greatly affected by seasonal variations in air temperatures, characteristic of frequent fluctuations and complex patterns of variation (Lunardini et al., 1995). In the permafrost region, coupling among environmental conditions, thermal properties, phase change, ground ice, and cryoturbation make the amplitude of the seasonal cycle increasingly attenuate with depth until approaching undetectable temperature variation at a depth of annual zero amplitude. (Less than instrument measurable accuracy, generally with the range of 0.1°C, and at 10–20 m on the QTP) (Jin et al., 2011; Dobiński, et al., 2022). Such that the ground is a natural low-pass filter of the short-term meteorological signal. Decadal or longer time-scale climate variations trend (the ‘signal’), however, can penetrate to deeper permafrost and hence be retained, which records past temperature changes at the ground surface (Romanovsky, 2010; Biskaborn,2019). Thus, the variations trend of mean annual ground temperature at the depths of zero annual amplitude is generally consistent with the long-term trend of air temperature while the distribution of warming

during the year has little effect on long-term permafrost degradation (Smith and Riseborough, 1983; Buteau et al., 2004; Biskaborn,2019). As mentioned above, here, the focus of this study is to discuss the long-term trend of the permafrost temperature over the foreseeable future. Because of a linearly warming trend is projected in mean annual air temperature over the QTP during the 21st century under different climate change scenarios, and a strong linear relationship between GST and AT over our study area. Hence, forcing data (land surface temperature) to increase linearly in the future in our work cannot affect the long-term variations trend of permafrost temperature.

In the revised manuscript, we have made a supplement to the description of the current limitation in projection of permafrost degradation and future improvements in the discussion section. The text there reads as: "*The limitation of this study includes that projected the possible fate of permafrost over Xidatan by 2100, under an area-mean warming rate scenario of QTP. Hence, the anticipated permafrost degradation in this study, may not be the actual overview, as it does not consider the regional-level or small-scale-based future climate change, but our simulation results can provide a relatively reasonable projection indication of the permafrost degradation levels over marginal permafrost on the QTP under the different climate change scenarios in the foreseeable future. High-resolution climate models and improved numerical representations of atmospheric circulation systems and land-atmosphere interactions over the heterogeneous QTP region could be a crucial step toward improving the GCMs/RCMs performance, thereby accuracy in the projection of permafrost degradation in the future.*"

Reference:

Lun, Y., Liu, L., Cheng, L., Li, X., Li, H., and Xu, Z.: Assessment of GCMs simulation performance for precipitation and temperature from CMIP5 to CMIP6 over the Tibetan Plateau, Int J Climatol. 41: 3994–4018. https://doi.org/10.1002/joc.7055,2021.

Cui, T., Li, C., and Tian, F.: Evaluation of temperature and precipitation simulations in CMIP6 models over the Tibetan Plateau, Earth and Space Science, 8, e2020EA001620. https://doi.org/10.1029/2020EA001620, 2021.

You, Q., Cai, Z., Wu, F., Jiang, Zhi., Pepin, N., and Shen, S.: Temperature dataset of CMIP6 models over China: evaluation, trend and uncertainty, Clim Dyn 57, 17–35https://doi.org/10.1007/s00382-021-05691-2, 2021.

Zhu, Y., and Yang, S.: Evaluation of CMIP6 for historical temperature and precipitation over the Tibetan Plateau and its comparison with CMIP5, Adv Clim Chang Res 11, 239–251, https:// doi. org/10. 1016/j. accre. 2020. 08. 001, 2020.

Jia, K., Rua, Y., Yang, Y., and You, Z.: Assessment of CMIP5 GCM simulation performance for temperature projection in the Tibetan Plateau, Earth and Space Science, 6, 2362-2378. https://doi.org/10.1029/2019EA000962, 2019.

Chen, X., Liu, Y., and Wu, G., Understanding the surface temperature cold bias in CMIP5 AGCMs over the Tibetan Plateau, Adv. Atmos. Sci. 34, 1447-1460, https://doi.org/10.1007/s00376-017-6326-9, 2017.

Hu, Q., Jiang, D., and Fan. G.: Evaluation of CMIP5 models over the Qinghai-Tibetan Plateau, Chin. J. Atmos. Sci, 38: 924-938, 2014.

Su, F., Duan, X., Chen, D., Hao, Z., and Cuo, L.: Evaluation of the global climate models in the CMIP5 over the Tibetan Plateau. J. Climate, 26, 3187–3208, https://doi.org/10.1175/JCLI-D-12-00321.1, 2013.

Zhu, X., Wang, W., and Fraedrich, K.: Future climate in the Tibetan Plateau from a statistical regional climate model, J. Climate, 26, 10125-10138, https://doi.org/10.1175/JCLI-D-13-00187.1, 2013.

Gao, X., Shi, Y., Song, R., Giorgi, F., Wang, Y., and Zhang, D.: Reduction of future monsoon precipitation over China: Comparison between a high-resolution RCM simulation and the driving GCM, Meteorol. Atmos. Phys., 100, 73–86, doi:10.1007/s00703-008-0296-5, 2008.

Lunardini, V.: Permafrost Formation Time. CRREL Report 95-8, US Army Corps of Engineers, Cold Regions Research and Engineering Laboratory, 1995.

Dobiński, W., and Marek K.: Permafrost Base Degradation: Characteristics and Unknown Thread With Specific Example From Hornsund, Svalbard, Front. Earth Sci. 10:802157, doi: 10.3389/feart.2022.802157, 2022.

Romanovsky, V., Oberman, N., Drozdov, D., Malkova, G., Kholodov, A., and Marchenko, S.: Permafrost, in Changes in the Arctic: Background and Issues, 80-82, 2010.

Iturbide, M., Gutiérrez, J., Alves, L., Bedia, J., Cerezo-Mota, R., Cimadevilla, E., Cofiño, A., Di, L., Faria, S., Gorodetskaya, I., Hauser, M., Herrera, S., Hennessy, K., Hewitt, H., Jones, R., Krakovska, S., Manzanas, R., Martínez-Castro, D., Narisma, G., Nurhati, I., Pinto, I., Seneviratne, S., van den Hurk, B., and Vera, C.: An update of IPCC climate reference regions for subcontinental analysis of climate model data: definition and aggregated datasets, Earth Syst. Sci. Data, 12, 2959–2970, https://doi.org/10.5194/essd-12-2959-2020,2020

IPCC. Climate change 2021: the physical science basis, https://www.ipcc.ch/report/ar6/wg1/downloads/report/IPCC_AR6_WGI_Full_Report.pdf., 2021.

Noetzli, J., Matthes, H., Vieira, G., Streletskiy, D., Schoeneich, P., Romanovsky, V., Lewkowicz, A., Abramov, A., Allard, M., Boike, J., Cable, W., Christiansen, H., Delaloye, R., Diekmann, B., Drozdov, D., Etzelmüller, B., Grosse, G., Guglielmin, M., Ingeman-Nielsen, T., Isaksen, K., Ishikawa, M., Johansson, M., Johannsson, H., Joo, A., Kaverin, D., Kholodov, A., Konstantinov, P., Kröger, T., Lambiel, C., Lanckman, J., Luo, D., Malkova, G., Meiklejohn, I., Moskalenko, N., Oliva, M., Phillips, M., Ramos, M., Sannel, A., Sergeev, d., Seybold, C., Skryabin, P., Vasiliev, A., Wu, Q., Yoshikawa, K., Zheleznyak, M., Lantuit, H.: Permafrost is warming at a global scale. Nat Commun 10, 264, https://doi.org/10.1038/s41467-018-08240-4, 2019.

Smith, M., Riseborough, D.: Permafrost sensitivity to climatic change. In Proceedings, 4th International Conference on Permafrost, Vol. 1. Fairbanks, Alaska, National Academy Press:

Washington, DC; 1178–1183, 1983.

Buteau, S., Fortier, R., Delisle, G., and Allard, M.: Numerical simulation of the impacts of climate warming on a permafrost mound, Permafrost and Periglac. Process., 15, 41-57, https://doi.org/10.1002/ppp.474, 2004.

Jin, H., Luo, D., Wang, S., Lü, L., and Wu, J.: Spatiotemporal variability of permafrost degradation on the Qinghai-Tibet Plateau, Sci. Cold Arid Reg., 3, 281–305, DOI: 10.3724/SP.J.1226.2011.00281, 2011.

2. For the methods of spatially modeling (Section 2.3.4), how the authors obtain the soil stratigraphy in the area without any borehole, e.g., 35°40' N - 35°42', because the authors pointed out that "the well-adjusted thermos-physical parameters of multilayered soil columns during the model calibration were specified and assigned for each grid cell of the same soil classes in the surrounding areas of the calibrating borehole".

Response:

In our work, the soil stratigraphy in the area without any boreholes was defined based on the surficial soil type maps at 1km × 1km spatial resolution. The map is mainly based on the relationships between environmental factors and soil types in the permafrost region of the QTP by applying a decision-making tree to spatialize the soil types (Li et al., 2014, 2015b). The results exhibited good reliability and thus could be used to realize the spatialization of soil thermal properties (Zou et al., 2017). The horizontal resolution of the simulation was 1km×1km, and the model domain ranged from 35°42′N to 35°45′N and from 94°3′E to 94°15′E, and encompasses an area of 280 km^2.We collected as many as fifteen monitoring boreholes with long-term temperature observation established in the Xidatan, which were specific for each soil type class and geographical location. Thermophysical properties (e.g., stratigraphies, texture, ground ice content, organic matter content, dry bulk density) of distinct soil layers were measured or assessed for field surveys, laboratory, and on-site measurement, as well as tests on soil samples obtained from fifteen borehole cores (depth between 8~30 m). Based on these properties, we calibration thermophysical parameters of different soil layers, then, well–adjusted thermos–physical parameters of multilayered soil columns were assigned for each soil type for spatial modeling.

To be clear, we have stated in the revised manuscript that *"Based on the soil type map at 1km×1km spatial resolution, well–adjusted thermos–physical parameters of multilayered soil columns in section 2.3.2 were specified and assigned for each soil type."*

Reference:

Li, W., Zhao, L., Wu, X., Zhao, Y., Fang, H., and Shi, W.: Distribution of soils and landform relationships in the permafrost regions of Qinghai-Xizang (Tibetan) Plateau, Chinese Sci. Bull., 60, 2216–2226, https://doi.org/10.1360/N972014-01206, 2015b.

Zou, D., Zhao, L., Sheng, Y., Chen, J., Hu, G., Wu, T., Wu, J., Xie, C., Wu, X., Pang, Q., Wang, W., Du, E., Li, W., Liu, G., Li, J., Qin, Y., Qiao, Y., Wang, Z., Shi, J., and Cheng, G.: A new

map of permafrost distribution on the Tibetan Plateau, The Cryosphere, 11, 2527–2542, https://doi.org/10.5194/tc-11-2527-2017, 2017.

3. I suggested the authors should be better replot Fig 2-5, because it is hard for me to see the model's performance.

Response:

We have replotted Fig. 2-5 to make the contrast clearer, and shown as follows.

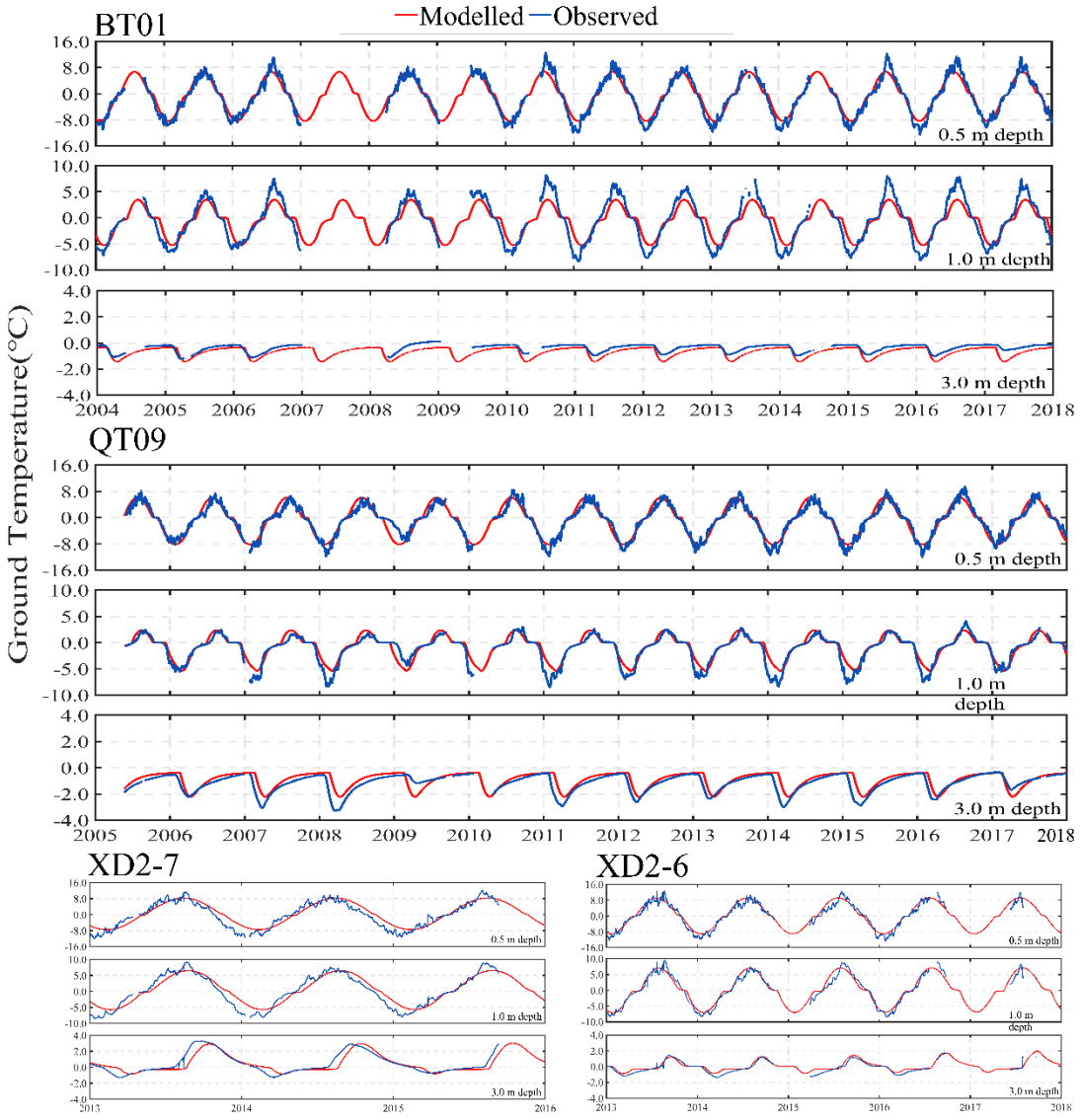

Figure 2. Comparison of the modelled (red lines) to observed (blue lines) daily mean ground temperature at 0.5 m, 1.0 m, 3.0 m depth in four calibration boreholes (BT01, XD2-7, QT09, and XD2-6) during the observation period (There were some data gaps due to temperature probe failure in some years, at the BT01, the data gaps in the record mainly occurred at 0.5-15 m in 2007-2008, and at 15-30 m during the 2005-2007 and 2011-2018, at the QT09, observations at 15-30 m of 2006-2008, 2011-2013, and 2015-2018 are not available, at the XD2-6, the data gap

in the record in 2016-2017).

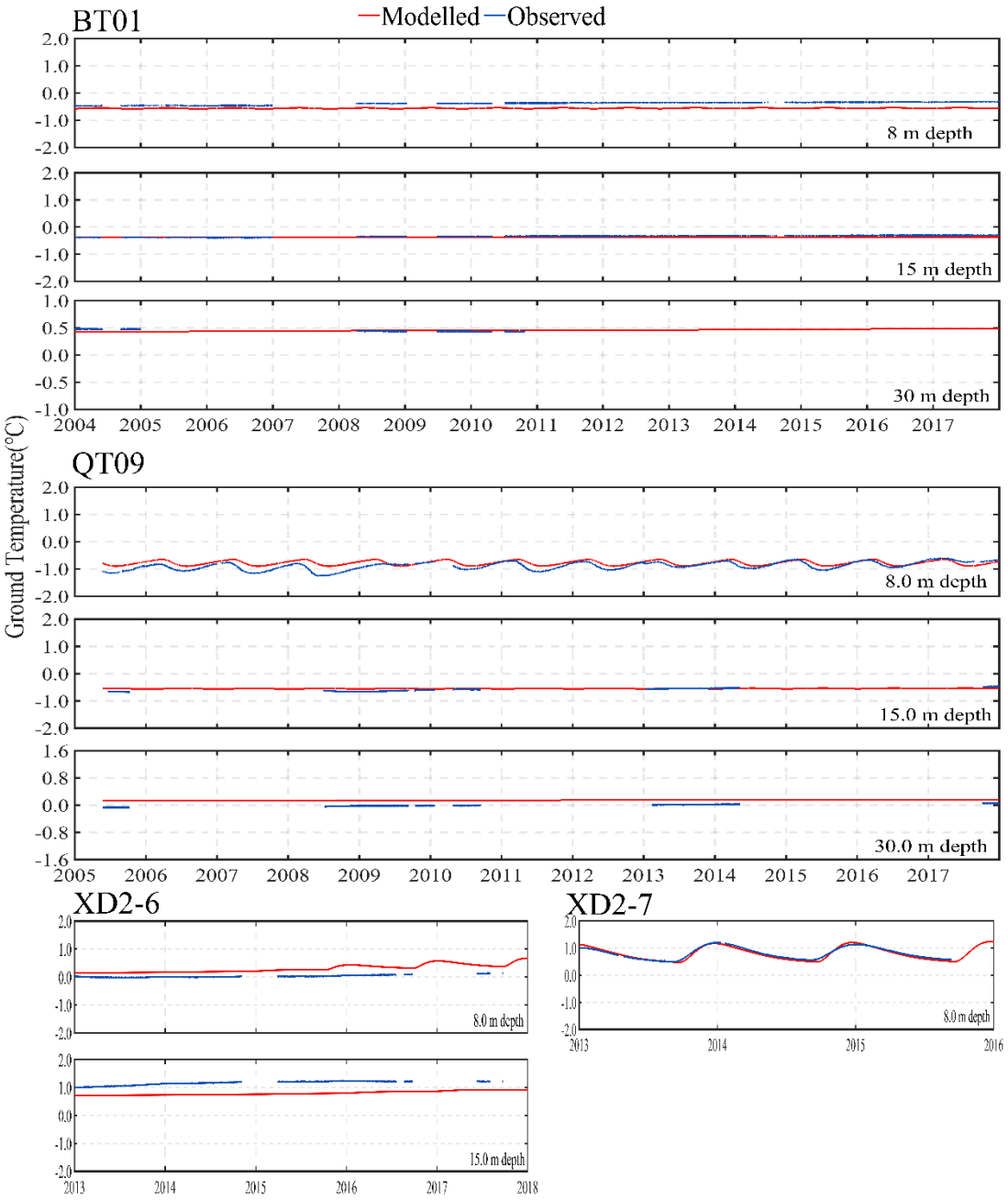

Figure 3. Same as Figure 2. but for daily mean ground temperature at 8 m, 15 m, and 30 m.

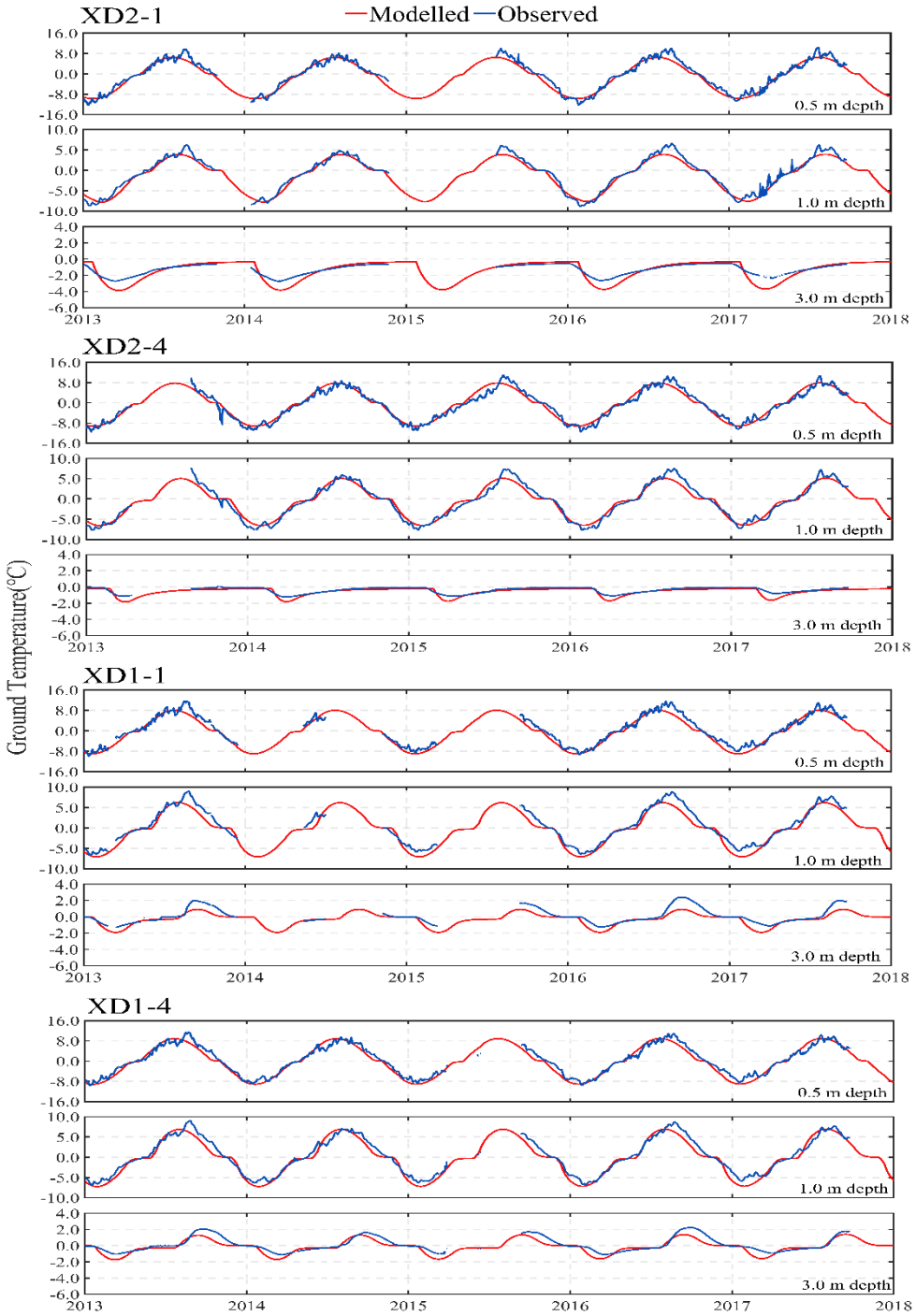

Figure 4. Comparison of the simulated (red lines) to observed (blue lines) daily mean ground temperature at 0.5 m, 1.0 m, and 3.0 m depth in four validation boreholes (XD2-1, XD2-4, XD1-1, and XD1-4) during the observation period from 2013 to 2018 (There were some data gaps due to temperature probe failure in some years, at the XD2-1, the data gaps in the record mainly occurred at 0.5-3.0 m in the first half of 2015. At the XD1-1, the data gap in the record at 0.5-3.0 in 2014-2015, at 8-15 m during the 2013-2015. At the XD1-4, the data gap in the record in the first half of 2015).

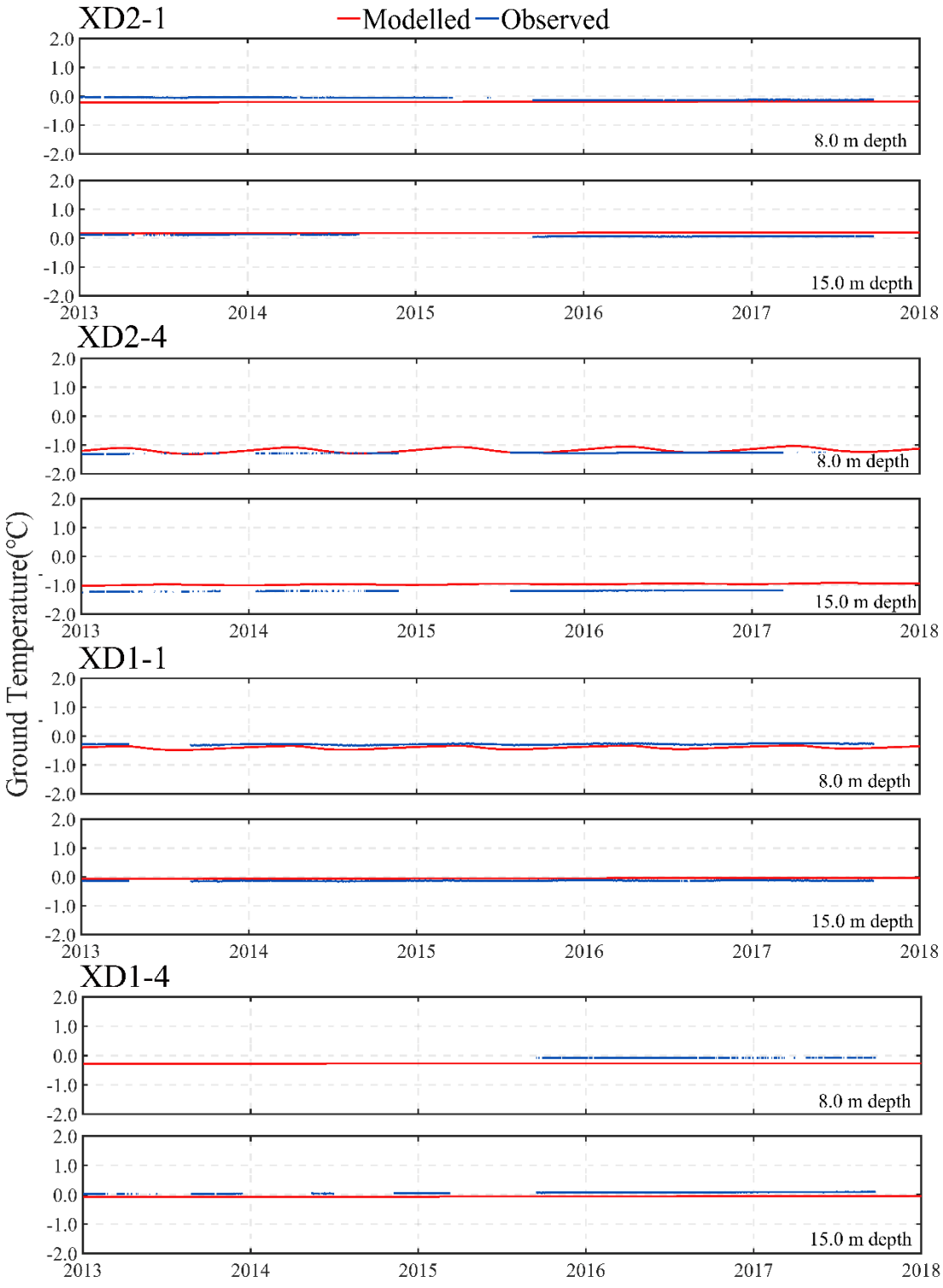

Figure 5. Same as Figure 4. But for daily mean ground temperature at 8 m, and 15 m.

4. For the third paragraph of section 4.2, the authors cited some projection studies that used statistical methods to detect the permafrost state in the future. But, as far as I know, there are existed some studies using the land surface model to simulate the permafrost change over the Tibetan Plateau, e.g., Guo et al., (2012), Qin et al., (2017), and Zhang et al., (2022). Therefore, what is the advantage of the model used in this manuscript compared to other numerical

transient models?

Response:

Thank you very much for the literature, we read it carefully.

Qin et al. (2012) also used the one-dimensional heat conduction permafrost model (GIPL) modeling of the active layer thickness and permafrost thermal state across QTP. But it does not consider ground thermal dynamics and is for equilibrium conditions, and no projection. By contrast, our simulation integrated climate and ground condition variables to quantify the change in permafrost under current and future climate change.

For Land Surface Lands (LSMs), Guo et al. (2012) used the Community Land Model4 (CLM4) to project that an approximately 81% reduction in near surface (<4.5 m) permafrost area on the QTP by the end of the 21st century under the A1B emission scenario. Additionally, the deep permafrost depths of 10 and 30m would be largely degraded by the year 2030-2050. Zhang et al. (2022) applied Noah LSM to project much of 44 ± 4%, 59 ± 5%, and 71 ± 7%, the permafrost is likely to degrade in the late 21st century, under SSP2-4.5, SSP3-7.0, and SSP5-8.5 scenarios, respectively, by 2100. These results and our simulation results unanimously revealed that further permafrost degradation tend was projected over the QTP under warm scenarios, but with a considerable discrepancy among these results on the magnitude of permafrost degradation. This discrepancy can, in part, be attributed to deficits of LSMs. Most of those LSMs were originally developed for shallow soil simulation, and the subsequent studies mainly focused on optimizing parameterization schemes and simply extending the soil column simulation depth, but they were poor with regard to considering the effecting of ground ice, thermal state of deep permafrost and geothermal heat flux (Sun et al. 2019, Lee et al., 2014). For example, ignoring the geothermal heat flux by setting zero flux or constant temperature as the bottom boundary condition (Wu et al., 2010; Xiao et al., 2013). However, these factors play a crucial role in the long-term evolution of permafrost in general (Xiao et al., 2013; Wu et al., 2010; Lee et al., 2014). Thus, the relationship between the decrease in the areal extent of permafrost and the warming air temperature over the present-day permafrost region is approximately linear simulated by LSMs. Given that such high rates of permafrost loss are not observed, this indicates a too-high sensitivity for those models predicting such losses (Zhao et al., 2020).

In comparison, our model considers the thermal property difference between frozen and thawed soil, the phase variations of the unfrozen water in frozen soil, the distribution of the ground ice, and geothermal heat flow. Thereby, can well describe the heat transfer process in permafrost and reasonably capture the attenuation and time lag of heat transfer in deep permafrost as water or ice content and ground is a poor conductor of heat. Moreover, our model is characterized by vertical modeling domains of one hundred meters with a vertical resolution of 0.05m within the active layer (the upper 4 m) and provides sufficient accuracy to resolve the annual dynamics of active layer thawing and refreezing, as well as the evolution of ground temperature in deeper layers. Our simulation results were reasonable and in compliance with observed facts. Moreover, the magnitude and evolution of permafrost degradation projection on the QTP derived our transient simulations agree well with that of the heat conduction permafrost model account for the thermal state of deep

ground ice (Li et al., 1996; Li et al., 2008; Sun et al., 2019). It can be noted that existing LSMs simulations largely ignore the thermal properties of deep permafrost, but our findings highlight initial permafrost thermal state is influenced by historical climate, stratigraphy thermal properties, ground ice distribution, geothermal heat flow, and propagation of the phase-transition interface plays a critical role in permafrost degradation.

In the revised manuscript, we have added a discussion about what is the advantage of the model used in this manuscript compared to other numerical transient models (e.g., LSMs) in section 4.2. these studies have been cited in the revised manuscript as follows. *"For Land Surface Lands (LSMs), Guo et al. (2012) used the Community Land Model4 (CLM4) to projects that an approximately 81% reduction in near surface (<4.5 m) permafrost area on the QTP by the end of the 21st century under the A1B emission scenario. Additionally, the deep permafrost depths of 10 and 30m would be largely degraded by the year 2030-2050. Zhang et al. (2022) applied Noah LSM to project much of 44 ± 4%, 59 ± 5%, and 71 ± 7%, the permafrost is likely to degrade in the late 21st century, under SSP2-4.5, SSP3-7.0, and SSP5-8.5 scenarios, respectively, by 2100."*

Reference

Qin, Y., Wu, T., Zhao, L., et al. 2017. Numerical modeling of the active layer thickness and permafrost thermal state across Qinghai-Tibetan Plateau. 122, 11604-11620. Journal of Geophysical Research: Atmospheres. https://doi.org/10.1002/2017JD026858.

Guo, D., Wang, H., Li, D. 2012. A projection of permafrost degradation on the Tibetan Plateau during the 21st century. 117, D05106. Journal of Geophysical Research: Atmospheres. https://doi.org/10.1029/2011JD016545.

Zhang, G., Nan, Z., Hu, N., et al. 2022. Qinghai-Tibet Plateau permafrost at risk in the late 21st Century. Earth's Future. 10, e2022EF002652. https://doi.org/10.1029/2022EF002652.

Sun, Z., Zhao, L., Hu, G., Qiao, Y., Du, E., Zou, D., Xie, C.: Modeling permafrost changes on the Qinghai-Tibetan plateau from 1966 to 2100: a case study from two boreholes along the Qinghai-Tibet engineering corridor. Permafrost and Periglac. Process., 32:156-171, https://doi.org/10.1002/ppp.2022, 2019.

Zhao, L., Zou, D. Hu, G., Du, E., Pang, Q., Xiao, Y., Li, R., Sheng, Y., Wu, X., Sun, Z., Wang, L., Wang, C., Ma, L., Zhou, H., and Liu, S.: Changing climate and the permafrost environment on the Qinghai–Tibet (Xizang) Plateau, Permafrost Periglac., 31, 396–405, https://doi.org/10.1002/ppp.2056, 2020.

Wu, Q., Zhang, T., and Liu, Y.: Permafrost temperatures and thickness on the Qinghai-Tibet Plateau, Global Planet. Change., 72, 32-38, https://doi.org/10.1016/j.gloplacha.2010.03.001, 2010.

Xiao, Y., Zhao, L., Dai, A., Li, R., Pang, Q., Yao, J.: Representing permafrost properties in CoLM for the Qinghai–Xizang (Tibetan) Plateau, 87, 68-77, https://doi.org/10.1016/j.coldregions.2012.12.004, 2013.

Hanna Lee, H., Swenson, S., Slater, A., and Lawrence, D.: Effects of excess ground ice on

projections of permafrost in a warming climate, Environ. Res. Lett. 9 124006, doi:10.1088/1748-9326/9/12/124006, 2014.

Li, S., Cheng, G., and Guo, D.: The future thermal regime of numerical simulating permafrost on the Qinghai-Xizang (Tibet) Plateau, China, under a warming climate. Science in China, Ser. D, 434-441,1996.

Li, D., Chen, J., Meng, Q., Liu, D., Fang, J., and Liu, J.: Numeric simulation of permafrost degradation in the eastern Tibetan Plateau, Permafrost and Periglac. Process., 19, 93-99, https://doi.org/10.1002/ppp.611,2008.

Specific comments

1. I do not see any citations for Table 2 and Table 3 in the manuscript.

Response:

The values of the thermal conductivity and heat capacity were from:

Yershov, E.: Principles of Geocryology (in Chinese), Lanzhou University Press, Lanzhou, China, 2016 (pp. 207-215).

Construction Ministry of PRC.: Code for design of soil and foundation of building in frozen soil region (in Chinese), China Architecture and Building Press, Beijing, China, 2011 (pp. 86-91), S86-S91.

附录K　冻土、未冻土热物理指标的计算(值)

K.0.1　根据土的类别、天然含水量及干密度测定数值，冻土和未冻土的容积热容量、导热系数和导温系数可分别按表K.0.1-1～表K.0.1-4取值。大含水(冰)量土的导热系数在无实测资料时可按表K.0.1-5取值。

草炭粉质粘土计算热参数值　　表K.0.1-1

ρ_d (kg/m³)	w (%)	C_u (kJ/m³·℃)	C_f (kJ/m³·℃)	λ_u (W/m·℃)	λ_f (W/m·℃)	$\alpha_u \cdot 10^3$ (m²/h)	$\alpha_f \cdot 10^3$ (m²/h)
400	30	903.3	710.9	0.13	0.13	0.50	0.62
	50	1237.9	878.2	0.19	0.22	0.52	0.92
	70	1572.4	1045.5	0.23	0.37	0.54	1.26
	90	1907.0	1212.8	0.29	0.53	0.56	1.59
	110	2241.6	1380.1	0.35	0.72	0.57	1.87
	130	2576.1	1547.3	0.41	0.88	0.57	2.06
500	30	1129.1	890.8	0.17	0.17	0.54	0.69
	50	1547.3	1099.9	0.24	0.31	0.56	1.30
	70	1965.5	1309.0	0.32	0.51	0.59	1.40
	90	2383.7	1518.1	0.41	0.74	0.61	1.76
	110	2801.9	1727.2	0.49	1.00	0.62	2.08
	130	3220.0	1936.3	0.56	1.24	0.63	2.31
600	30	1355.0	1066.4	0.22	0.22	0.57	0.76
	50	1856.8	1317.3	0.31	0.42	0.61	1.15
	70	2358.5	1568.3	0.42	0.68	0.64	1.56
	90	2860.5	1819.2	0.53	0.99	0.67	1.95
	110	3362.3	2070.1	0.63	1.32	0.68	2.29
	130	3864.2	2321.0	0.75	1.61	0.68	2.51

续表

(kg/m³) ρ_d	(%) w	(kJ/m³·℃) C_u	(kJ/m³·℃) C_f	(W/m·℃) λ_u	(W/m·℃) λ_f	(m²/h) $a_u \cdot 10^3$	(m²/h) $a_f \cdot 10^3$
700	30	1580.8	1246.2	0.27	0.30	0.61	0.87
	50	2166.3	1539.0	0.39	0.56	0.66	1.30
	70	2375.4	1831.7	0.53	0.88	0.70	1.74
	90	3337.2	2124.5	0.66	1.26	0.71	2.14
	110	3922.7	2417.2	0.79	1.67	0.73	2.50
	130	4508.2	2709.9	0.92	2.01	0.73	2.77
800	30	1806.6	1421.9	0.32	0.37	0.65	0.94
	50	2475.7	1756.4	0.48	0.68	0.70	1.41
	70	3144.9	2091.0	0.64	1.09	0.73	1.67
	90	3814.0	2425.6	0.80	1.55	0.76	2.32
	110	4483.1	2760.1	0.96	2.05	0.77	2.68
	130	5152.2	3094.7	1.10	2.47	0.78	2.88
900	30	1171.0	1342.4	0.38	0.40	0.68	1.03
	50	2785.2	1978.1	0.57	0.73	0.73	1.53
	70	3538.0	2354.5	0.75	1.14	0.77	2.03
	90	4290.7	2370.8	0.95	1.63	0.80	2.49
	100	5043.5	3107.2	1.14	2.12	0.82	2.86
	130	5796.3	3483.6	1.32	2.52	0.82	3.02

注：① 表中符号：ρ_d—干密度；w—含水量；λ—导热系数；C—容积热容量；a—导温系数；脚标：u—未冻土，f—已冻土。下同；

②表列数值可直线内插。

粉土、粉质粘土计算热参数值　　表 K.0.1-2

(kg/m³) ρ_d	(%) w	(kJ/m³·℃) C_u	(kJ/m³·℃) C_f	(W/m·℃) λ_u	(W/m·℃) λ_f	(m²/h) $a_u \cdot 10^3$	(m²/h) $a_f \cdot 10^3$
1200	5	1254.6	1179.3	0.25	0.26	0.73	0.76
	10	1505.5	1405.2	0.43	0.41	1.02	1.04
	15	1756.4	1530.6	0.58	0.58	1.19	1.37
	20	2007.4	1656.1	0.67	0.79	1.21	1.71
	25	2258.3	1781.5	0.72	1.04	1.14	2.10
	30	2509.2	1907.0	0.79	1.28	1.13	2.40
	35	2760.1	2032.5	0.86	1.45	1.12	2.57

续表

(kg/m³) ρ_d	(%) w	(kJ/m³·℃) C_u	(kJ/m³·℃) C_f	(W/m·℃) λ_u	(W/m·℃) λ_f	(m²/h) $a_u \cdot 10^3$	(m²/h) $a_f \cdot 10^3$
1300	5	1359.2	1279.7	0.30	0.29	0.80	0.80
	10	1631.0	1522.2	0.50	0.48	1.11	1.12
	15	1902.8	1660.3	0.71	0.71	1.33	1.47
	20	2174.6	1794.1	0.79	0.92	1.31	1.85
	25	2446.5	1932.1	0.84	1.21	1.23	2.25
	30	2718.3	2065.9	0.90	1.46	1.19	2.55
	35	2990.1	2203.9	0.97	1.67	1.18	2.74
1400	5	1463.7	1375.9	0.36	0.35	0.87	0.90
	10	1756.4	1639.3	0.59	0.57	1.22	1.22
	15	2049.2	1785.7	0.84	0.79	1.46	1.58
	20	2341.9	1932.1	0.94	1.06	1.44	1.96
	25	2634.7	2496.7	0.97	1.39	1.33	2.41
	30	2927.4	2224.8	1.06	1.68	1.32	2.73
	35	3220.1	2371.2	1.18	1.93	1.32	2.92
1500	5	1568.3	1476.2	0.41	0.41	0.93	0.98
	10	1881.9	1756.4	0.67	0.65	1.28	1.32
	15	2191.4	1907.0	0.96	0.91	1.58	1.71
	20	2509.2	2070.1	1.09	1.22	1.57	2.12
	25	2822.9	2229.0	1.13	1.58	1.44	2.55
	30	3136.5	2383.7	1.24	1.89	1.43	2.85
	35	3450.2	2542.7	1.36	2.12	1.42	3.01
1600	5	1672.8	1572.4	0.46	0.46	1.01	1.05
	10	2425.6	1873.5	0.78	0.74	1.40	1.42
	15	2541.9	2040.8	1.11	1.02	1.72	1.81
	20	2676.5	2208.1	1.24	1.38	1.67	2.25
	25	3011.0	2375.4	1.28	1.80	1.52	2.73
	30	3345.6	2542.7	1.42	2.12	1.52	3.01
	35	3680.2	2709.9	1.54	2.40	1.51	3.20

碎石粉质粘土计算热参数值　　表 K.0.1-3

ρ_d (kg/m³)	w (%)	C_u (kJ/m³·℃)	C_f (kJ/m³·℃)	λ_u (W/m·℃)	λ_f (W/m·℃)	$\alpha_u \cdot 10^3$ (m²/h)	$\alpha_f \cdot 10^3$ (m²/h)
1200	3	1154.2	1053.9	0.23	0.22	0.72	0.77
	7	1355.0	1154.2	0.34	0.37	0.91	1.15
	10	1505.5	1229.5	0.43	0.52	1.03	1.52
	13	1656.1	1304.8	0.53	0.71	1.16	1.96
	15	1756.4	1355.0	0.59	0.85	1.21	2.26
	17	1856.8	1405.2	0.60	0.94	1.26	2.42
1400	3	1346.6	1229.5	0.34	0.32	0.89	0.97
	7	1568.3	1346.6	0.50	0.53	1.15	1.44
	10	1756.4	1434.4	0.65	0.74	1.33	1.86
	13	1932.1	1522.2	0.79	0.97	1.48	2.30
	15	2049.2	1580.8	0.88	1.14	1.55	2.59
	17	2166.3	1639.3	0.92	1.24	1.53	2.73
1600	3	1539.0	1405.2	0.46	0.45	1.07	1.17
	7	1806.6	1539.0	0.68	0.74	1.38	1.73
	10	2007.4	1639.3	0.89	1.00	1.61	2.20
	13	2208.1	1739.7	1.10	1.29	1.80	2.66
	15	2341.9	1806.6	1.28	1.45	1.87	2.90
	17	2475.7	1873.5	1.42	1.57	1.96	3.02
1800	3	1731.3	1580.8	0.60	0.60	1.25	2.38
	7	2032.5	1731.3	0.92	0.97	1.62	2.43
	10	2258.3	1844.3	1.17	1.31	1.87	2.56
	13	2295.9	1957.2	1.45	1.65	2.10	3.03
	15	2634.7	2032.5	1.60	1.82	2.19	3.23
	17	2785.2	2107.7	1.71	1.93	2.21	3.28

砾砂计算热参数值　　表 K.0.1-4

ρ_d (kg/m³)	w (%)	C_u (kJ/m³·℃)	C_f (kJ/m³·℃)	λ_u (W/m·℃)	λ_f (W/m·℃)	$\alpha_u \cdot 10^3$ (m²/h)	$\alpha_f \cdot 10^3$ (m²/h)
1400	2	1229.5	1083.1	0.42	0.49	1.23	1.62
	6	1463.7	1200.2	0.96	1.14	2.36	3.42
	10	1697.9	1317.3	1.17	1.43	2.40	3.91
	14	1932.1	1434.4	1.29	1.67	2.40	4.20
	18	2166.3	1551.5	1.39	1.86	2.27	4.31
1500	2	1317.3	1162.6	0.50	0.59	1.36	1.84
	6	1568.3	1288.1	1.09	1.32	2.51	3.70
	10	1819.2	1413.5	1.30	1.60	2.58	4.08
	14	2070.1	1539.0	1.44	1.87	2.51	4.38
	18	2321.0	1664.4	1.52	2.08	2.37	4.50
1600	2	1405.2	1237.9	0.61	0.73	1.56	2.13
	6	1672.8	1371.7	1.28	1.60	1.74	4.21
	10	1940.4	1505.5	1.48	1.86	2.75	4.44
	14	2208.1	1639.3	1.64	2.15	2.67	4.72
	18	4173.6	1773.2	1.69	2.35	2.47	4.79
1700	2	1493.0	1317.3	0.77	0.94	1.85	2.52
	6	1777.4	1459.5	1.47	1.91	2.99	4.73
	10	2061.7	1601.7	1.68	2.20	2.94	4.96
	14	2346.1	1743.9	1.84	2.48	2.84	5.13
	18	2630.5	1886.1	1.95	2.69	2.66	5.14
1800	2	1580.8	1392.6	0.95	1.19	2.17	3.09
	6	1881.9	1543.2	1.71	2.27	3.27	5.31
	10	2183.0	1693.7	1.91	2.61	3.17	5.56
	14	2484.1	1844.3	2.09	2.85	3.02	5.58
	18	2785.2	1994.8	2.18	3.05	2.82	5.51

大含水(冰)量土的导热系数　　表 K. 0. 1-5

红色粉质粘土				黄色粉土			
青海风火山				兰州			
(kg/m³)	(%)	(W/m·℃)		(kg/m³)	(%)	(W/m·℃)	
ρ_d	w	λ_u	λ_f	ρ_d	w	λ_u	λ_f
380	202.4	0.73	2.15	400	200.0	—	2.13
680	109.2	0.94	2.06	700	100.0	—	2.08
900	78.2	1.03	1.97	1000	55.8	—	2.05
1000	60.0	1.08	1.95	1200	40.0	1.94	2.02
1100	50.0	1.08	1.95	1400	35.0	1.86	1.91
1200	44.9	1.09	1.88	1400	30.0	1.72	1.81
1200	34.3	1.09	1.67	—	—	—	—
草炭粉土				草根(皮)			
西藏两道河				西藏两道河			
(kg/m³)	(%)	(W/m·℃)		(kg/m³)	(%)	(W/m·℃)	
ρ_d	w	λ_u	λ_f	ρ_d	w	λ_u	λ_f
100	960.0	—	1.86	100	840	—	1.62
200	428.8	—	2.16	200	400	0.68	1.86
300	300.0	—	2.25	200	300	0.57	1.32
300	284.4	—	1.98	200	250	0.46	0.86
400	180.8	—	2.03	200	200	0.39	0.65
500	143.3	—	2.06	200	150	0.27	0.46
700	138.1	—	2.13	200	100	0.23	0.26
—	—	—	—	300	250	0.65	1.65
—	—	—	—	300	180	0.45	1.07
—	—	—	—	300	150	0.41	0.93
—	—	—	—	300	130	0.36	0.68
—	—	—	—	300	110	0.36	0.57

2. L322-323: 0.032℃ a-1 (SSP2-4.5, moderate mitigation)?

Response:

It has been corrected in the revised manuscript. The text there reads as: "*0.032℃ a^{-1}(SSP2-4.5, moderate mitigation)*".

3. L326: RCP8.5?

Response:

The full text is thoroughly revised and carefully checked to delete errors.

4. Please keep the abbreviation of 'SSPx-y' consistently, e.g., some sentences use SSP1-2.6 (L322), and some sentences use SSP1-26 (L502).

Response:

It has been corrected to the 'SSPx-y.' format throughout the revised manuscript.